department of electrical engineering

AFCRL-72-0143

LASER PRODUCED DAMAGE IN TRANSPARENT SOLIDS

by
David F. Edwards and C. Y. She

Quantum Electronics Laboratory
Colorado State University
Fort Collins, Colorado 80521

Contract No. F19628-69-C-0197
Project, Task, and Work Unit No. 4645-07-01

Final Report
1 March 1969 - 30 September 1971

February 1972

Contract Monitor: Erlan S. Bliss, Captain, USAF

Optical Physics Laboratory

Prepared for

AIR FORCE CAMBRIDGE RESEARCH LABORATORIES
AIR FORCE SYSTEMS COMMAND
UNITED STATES AIR FORCE
BEDFORD, MASSACHUSETTS 01730

AFCRL-72-0143

LASER PRODUCED DAMAGE IN TRANSPARENT SOLIDS

by

David F. Edwards and C. Y. She

Quantum Electronics Laboratory
Colorado State University
Fort Collins, Colorado 80521

Contract No. F19628-69-C-0197

Project, Task, and Work Unit No. 4645-07-01

Final Report
1 March 1969 - 30 September 1971

February 1972

Contract Monitor: Erlan S. Bliss, Captain, USAF

Optical Physics Laboratory

Prepared for

AIR FORCE CAMBRIDGE RESEARCH LABORATORIES
AIR FORCE SYSTEMS COMMAND
UNITED STATES AIR FORCE
BEDFORD, MASSACHUSETTS 01730

ABSTRACT

The mechanism governing the onset of laser-produced damage in solids was found to depend, in a critical way, on the spatial and/or temporal gradient of the interaction strength across the focal volume. As a result, the threshold values of damage produced by a multimode laser as well as the internal damage patterns depend strongly on the laser propagation and polarization directions.

In the forward scattering experiment, the cumulative effects of microscopic damage were observed in crystalline quartz. Other experiments designed to detect cumulative effects were inconclusive. Various light scattering spectroscopy as a diagnostic tool for laser-produced damage studies were investigated.

TABLE OF CONTENTS

LIST OF TABLES

LIST OF FIGURES

I. INTRODUCTION

The primary objective of this research project has been to make an experimental and theoretical investigation of the criteria governing the onset of laser-produced damage in transparent solids. This research was concerned with the microscopic damage produced within the interior of the solid. Surface damage or internal macroscopic damage were not of primary concern for this program. The main tasks were as follows: to develop a diagnostic tool for studying microscopic damage, to determine the damage mechanism, and to establish the relationship of microscopic damage to macroscopic damage.

Under certain conditions an intense laser pulse transmitted through a transparent solid, such as a window or a lens, will produce damage internal to the solid. Within the laser rod itself, the laser pulse often produces damage leading to self-destruction of the rod. The damaged region appears as a "bubble" or a crack within the solid and this type of damage is generally called macroscopic or catastrophic damage. Laser-produced macroscopic damage has been observed in many laboratories using high-power laser systems. It is the catastrophic damage threshold value that often sets the design parameters of a laser system. Microscopic or pre-catastrophic damage is a local defect that alters the optical properties of the laser rod. This defect might be reversible or exist only during the lifetime of the laser pulse, for example, thermally induced refractive index change.

The defect may also be permanent and may accumulate or increase in size with successive laser pulses. A laser induced color center might be an example of this latter type defect. An important question is whether this microscopic damage will continue to grow with successive laser pulses until macroscopic damage is produced. Both the permanent- and cumulative-type microscopic damage are of concern for this research program.

During the past five years, several laboratories have given special attention to the macroscopic-damage problem; few have investigated microscopic damage. Because of the importance and the growing interest in the problem, in 1969 the American Society for Testing and Materials initiated annual symposia on laser-produced damage. Based on the reports [1-3] and

discussions presented at the symposia, it is evident that progress has been made but the damage mechanism remains unknown and is probably dependent on the material and conditions of the experiment. No commonly accepted picture of the damage mechanism has emerged. The results of this present research program have been reported[1-3] at each of the symposia and represent the only investigation of microscopic damage.

Given in Section II are the results of several experiments used to evaluate light-scattering spectroscopy as an effective diagnostic tool for investigating microscopic damage. Raman and Raleigh scattering by microscopically damaged quartz crystals were investigated. Stress induced defects in crystalline quartz was successfully studied[4] using Raman scattering. The Raman and fluorescence spectra were measured for ruby crystals having different chromium concentrations. The defects here are the chromium atoms in the sapphire (Al_2O_3) lattice. Primary results showed only limited success for ruby and, therefore, these experiments were terminated. Changes in the Raman linewidth were measured for laser-induced microscopic damage in crystalline quartz.

In Section III the results are given of experiments measuring the effects of laser-mode structure on the threshold value and pattern of macroscopic damage in crystalline quartz. Directional and polarization dependence relative to crystallographic axes were experimentally established for both the damage threshold value and the damage pattern. The observed dependences can be quantitatively explained in terms of electrostrictive interactions and acoustic wave propagation.

Experiments designed to measure the cumulative effects and the evolution of microscopic into macroscopic damage are described in Section IV. Measurements were conducted in fused quartz, laser glass, as well as crystalline quartz, using a TEM_{oo} ruby laser and a multimode ruby laser. Different results were obtained for the two laser systems. The results are summarized and a discussion is given in the final section.

II. LIGHT SCATTERING AS A DIAGNOSTIC TOOL

The principal diagnostic tool used to study microscopic damage in solids has been light scattering spectroscopy. This method was suggested

by the following arguments. A distortion within a crystal disturbs the local lattice periodicity and, in general, will produce a change in the electronic polarizability of the solid. When this happens, the light scattering properties of the solid will be altered. When the distortion is due to defects, either natural or induced, the Rayleigh scattering may be enhanced. A distortion due to induced strain in the solid would alter the vibrational properties of the crystal and produce an appreciable change in the line position and linewidth of the Raman spectrum. In the case of laser crystal such as ruby, induced defects or strain may alter the crystalline field of the active ion (Cr^{3+} in the case of ruby) affecting the fluorescence radiation from the crystal.

2.1 Stress-Induced Raman Spectra

To assess the feasibility of Raman scattering spectroscopy to detect local stress or strain that might be induced by a giant laser pulse, the following experiment was conducted. A sample of crystalline quartz was subjected to an uniaxial stress and the changes of the line position, linewidth, and line intensity for some of the strong Raman-active vibrations were measured for applied pressures up to about 3 k-bars.[4,6] These pressures are of the same order of magnitude as those expected from the giant laser pulse. The dependence of the changes in line position and linewidth for several lines are shown in Figure 1. The measured changes in line position were in good agreement with the values calculated from the valence-force model[5] that had been modified to include the effects of the anharmonic potential and applied stress. The results of these experiments were published elsewhere.[4,6]

Shown in Figure 2 are the raw data of the 128 cm^{-1} E vibration in quartz as a function of applied stress. From the figure the change in line position with stress is easily seen, but any change in linewidth is not discernible from these data because the linewidth is comparable to the spectrometer resolution. The stress induced changes in the linewidth are observed after the line broadening effects of the spectrometer have been subtracted from the raw data. A computer program was developed[7] for performing this deconvolution. The significance of this stress-induced

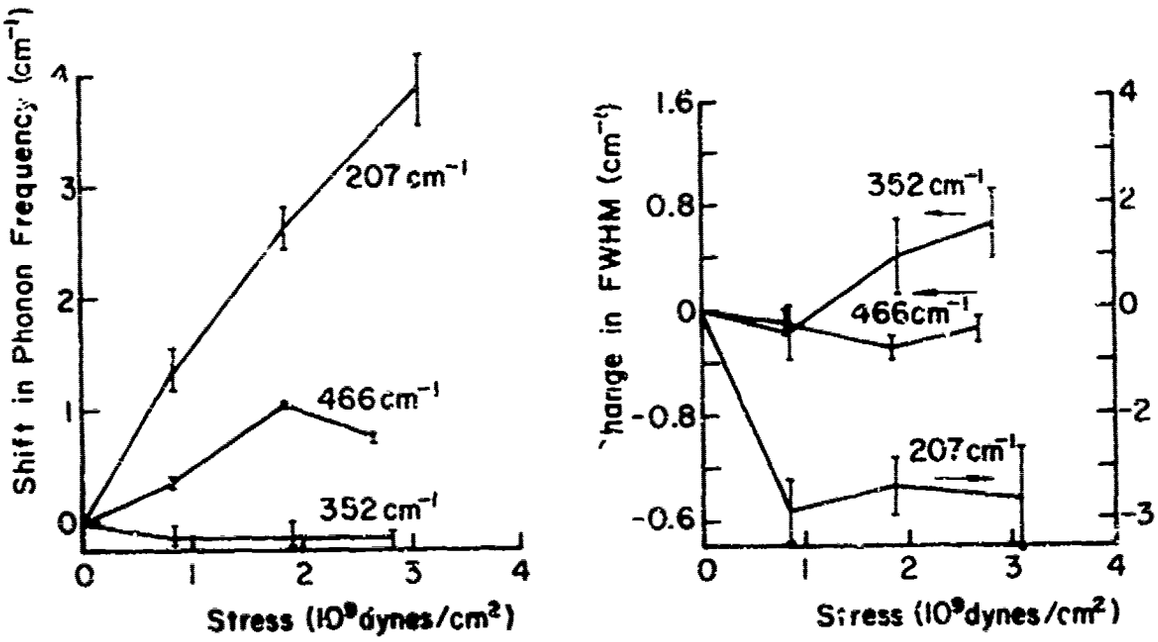

Fig. 1. Stress-dependent shifts in positions and widths in some of Raman active lines in α-quartz.

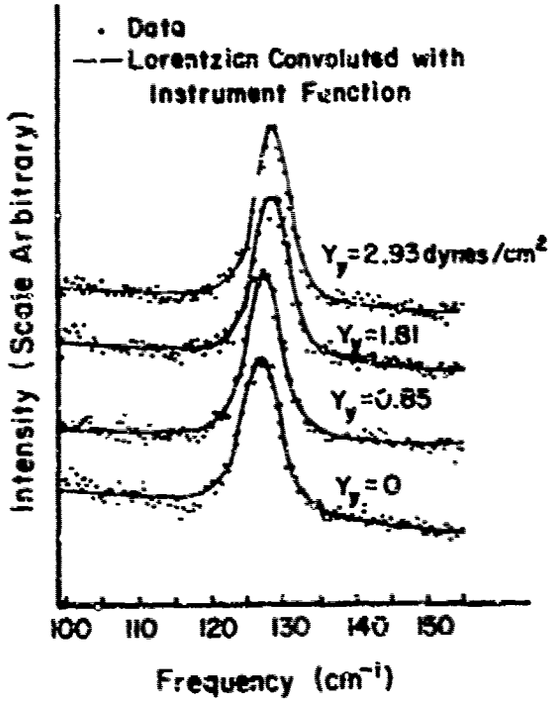

Fig. 2. Raw data showing the stress dependence of the 128 cm^{-1} line in α-quartz.

experiment was that changes in the Raman spectrum could be used for detecting locally induced stress. The experimental arrangement and details of the measurements were published elsewhere.[6,7]

2.2 Raman-Fluorescence Spectrum

Measurements were made of the He-Ne excited Raman-fluorescence spectrum of several ruby samples having different chromium concentrations. The purpose of this experiment was to determine the effect of the ionic additive on the Raman and fluorescence linewidths. Considering the Cr-ions as defects within the Al_2O_3 lattice, we were determining the feasibility of using Raman-fluorescence spectroscopy to detect changes in defect concentration. Furthermore, laser induced microscopic damage in ruby has been detected[8] as a change in the state of the Cr-ions. This change should be observed by a change in the fluorescence spectrum.

Shown in Figure 3 is an example of the Raman-fluorescence spectrum for a 0.05% ruby sample at 77°K. The notation (σ,σ) indicates that the excitation and scattered radiation were both polarized perpendicular to the plane defined by the optic axis of the crystal. From this and the spectra for the other orientations, the main features are the two strong lines at 14,199.4 cm^{-1} and 14,263.8 cm^{-1} corresponding to the N_1 and N_2, no-phonon, lines[9,10] and the ruby R-lines at 14,419.0 cm^{-1} and 14,488.0 cm^{-1}. In addition, there is evidence of 40 partially resolved lines on the low frequency side of the R lines. Most of these partially resolved lines have an associated line shifted 29 cm^{-1}, the same as the R-lines separation.

The measurements of the Raman-fluorescence spectrum of ruby were discontinued because of the lack of a liquid-helium temperature dewar. At room and liquid nitrogen temperatures the Raman-fluorescence spectra of ruby is very complex having relatively broad lines. At liquid helium temperatures these lines should become sharp,[9] permitting linewidth and lineshape analyses and the possible detection of changes in defect concentration.

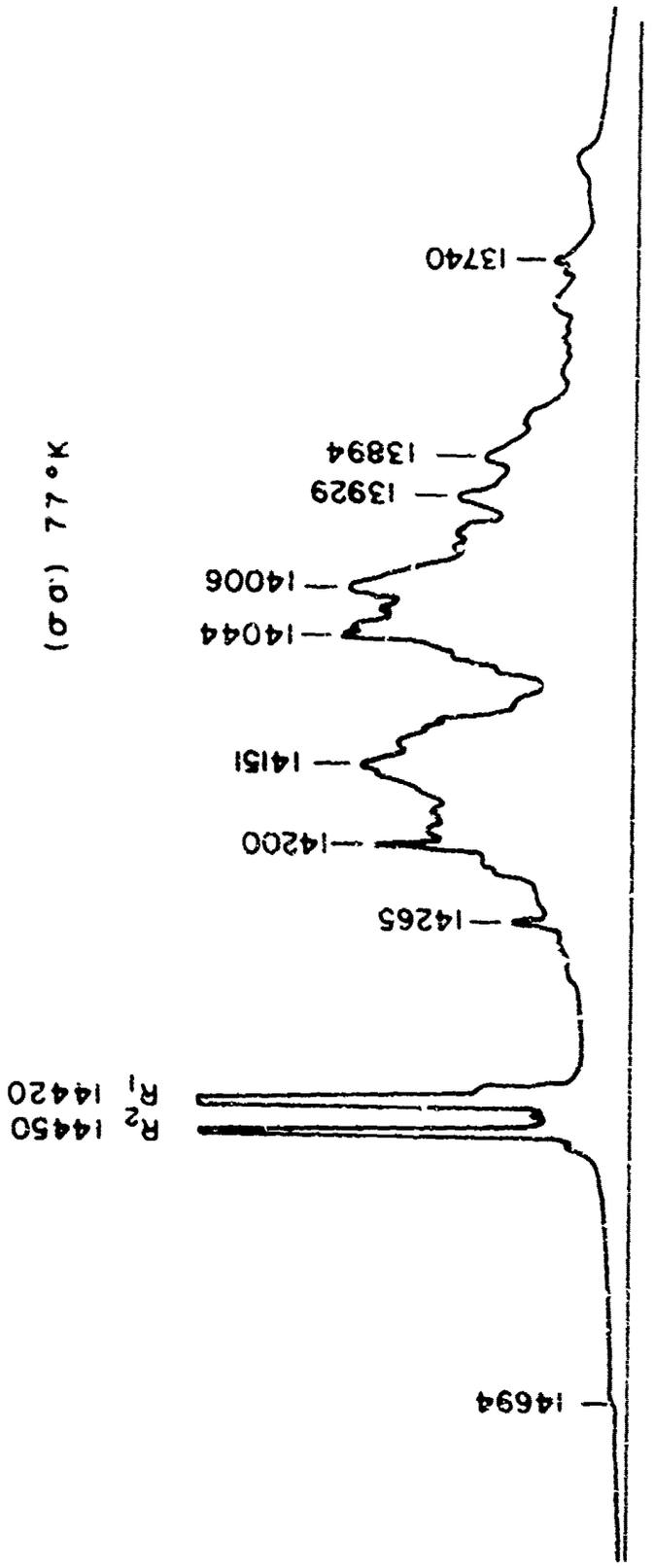

Fig. 3. The (σ,σ) fluorescence spectrum of ruby at 77°K.

2.3 Microscopic Damage in Quartz

The first evidence of laser-produced microscopic damage in crystalline quartz was the measured change in linewidth of the 128 cm^{-1} E-mode Raman line.[11] Macroscopic or catastrophic damage was produced in a quartz sample by a giant-pulsed ruby laser. The damage consisted of widely spaced bubbles with no evidence of damage between the bubbles when the sample was examined with side lighting. The Raman spectrum was measured in this region. It was found that the 128 cm^{-1} E-mode linewidth was about 20% broader than for an undamaged region Care was taken to mask off any light scattered from the bubble regions. This change in linewidth was interpreted to be evidence of microscopic damage and additional measurements were performed.

Two giant-pulsed lasers having different output characteristics were used for producing the damage. One laser was constructed such that the output was a single longitudinal mode and the lowest order transverse mode, TEM_{oo}. The output profile was verified to be TEM_{oo} by detailed probing of the laser near- and far-field patterns.[12] The output of the second laser was a single longitudinal mode but with several transverse modes. As a result several transverse modes could oscillate simultaneously during a laser pulse giving an irregular multimode beam profile. The microscopic damage produced by these two lasers was not the same and using the Raman spectrum as a microscopic probe, the following differences were observed: (1) For microscopic damage produced by the multi-mode laser, two "local modes" at about 550 cm^{-1} and 580 cm^{-1} were observed,[13] Fig. 4. Considerable effort was made to establish the origin of these two modes with the conclusion that they were associated with damage. Also, a peak at 189 cm^{-1} was originally thought to be a local mode was later found to be a neon line. To establish the origin of these local modes, it was necessary to make several modifications to the Raman spectrometer system. The most important modification was the substitution of a Double Czerny-Turner monochromator for a Littrow-mount instrument. (2) These new local modes at 550 cm^{-1} and 580 cm^{-1} were not observed for samples microscopically damaged by the TEM_{oo} laser. These new modes could be produced only with the multi-mode laser. (3) Careful measurement of the 207 cm^{-1} and the 466 cm^{-1} vibrations showed that within experimental error the line position and the linewidth

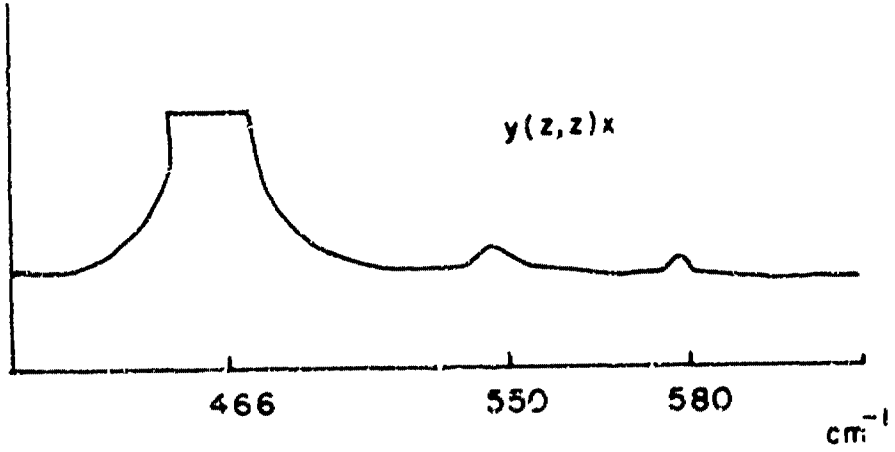

Fig. 4. The "local modes" observed in microscopically damaged α-quartz.

for both lines were independent of the number of laser pulses incident to the sample. The double monochromator was necessary for reaching this conclusion. Since the Raman spectrum was measured typically 30-60 minutes following the laser pulse, it was concluded that if a memory of microscopic damage exists in crystalline quartz, it is very small or it decays rapidly, perhaps in a time comparable to the laser pulse decay time. To test this rapid decay theory, the evolution experiment described in Section IV was performed.

III. LASER-MODE STRUCTURE EFFECTS

Measurements were made of the macroscopic damage properties of crystalline quartz for laser pulses having different mode structures. For a multimode laser pulse the catastrophic damage threshold value was found to depend on both the propagation and polarization directions of the incident radiation. The threshold value for damage produced by the TEM_{oo} laser was independent of direction. In addition to the different threshold values, the damage patterns were dependent on the direction of propagation.

The effects of the laser-mode structure on the macroscopic damage were measured for crystalline quartz using the TEM_{oo} laser and the multimode laser. Shown in Fig. 5 are isodensity contour plots of the energy distribution in the output beams of these two lasers. These contour plots were made by photographing the beam in the focal plane of the damage lens (fl=30 mm) using fine grain Kodak type 649-0 film. Shown in Fig. 5a are the smooth and approximately Gaussian distribution of the isodensity contour lines that are typical for the TEM_{oo} laser. The Fresnel number for this laser is about 0.67 so that the normalized spatial and temporal intensity distributions remain about the same during the pulse lifetime for this TEM_{oo} laser.[12] This being the case, the time integrated beam diameter at the $1/e^2$ intensity points of Fig. 5a was taken as the beam diameter for our experiments and corresponds to 50u. The full width at half maximum (FWHM) pulse width is 8 nsec for the TEM_{oo} laser pulse. The time integrated profile of the multimode laser, (MM), shown in Fig. 5b, has a diameter of about 275u. From the irregular contour lines it can be seen that the

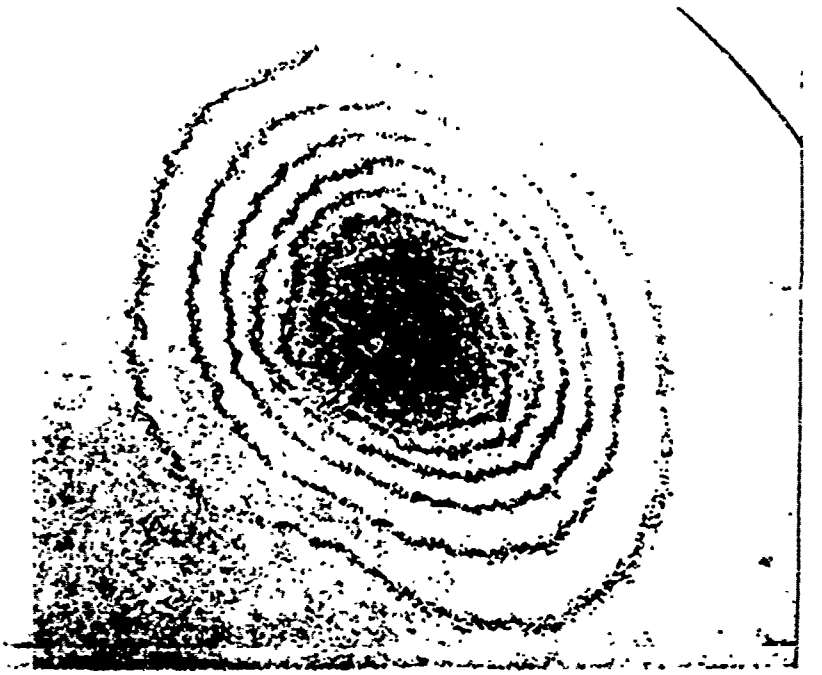

(5a). TEM_{oo} Laser

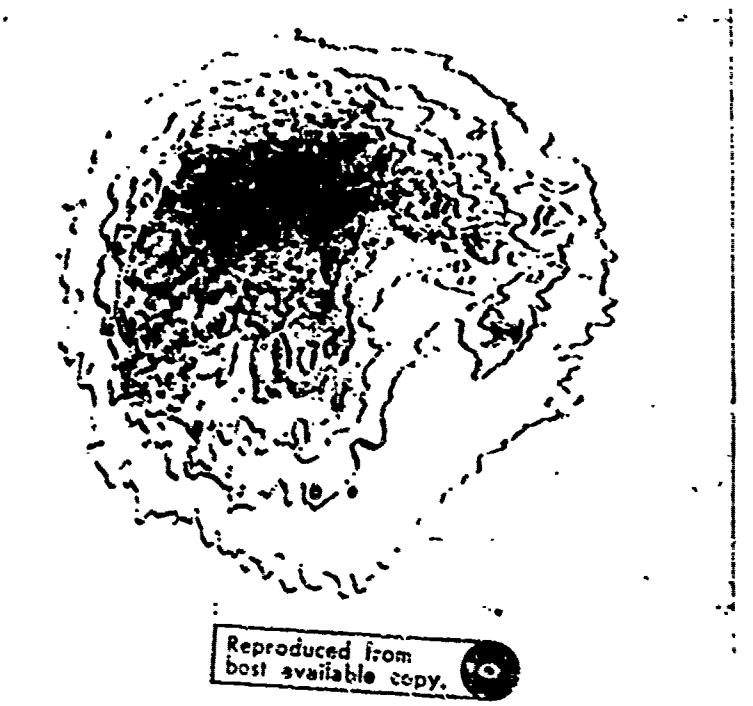

(5b). Multimode Laser

Fig. 5. Isodensity contour plots of the energy distribution in the output beams of the two lasers.

energy was nonuniformly distributed across the beam profile. These regions, sometimes called "hot spots," vary in space and time from pulse to pulse.[12] The space integrated FWHM pulse width was typically 20 nsec for the multimode laser. The Fresnel number for the multimode laser was about 93. The irregular spatial and temporal behavior for the MM laser output makes the analysis of data taken with this laser more complex than the analysis of data taken from the TEM_{oo} laser.

The experimental procedure was to focus the beam of either laser into a quartz sample that had been crystallographically oriented relative to the laser propagation and polarization directions. The focusing lens was the same one as used to produce Fig. 5. The peak power of the laser for each pulse was measured using a calibrated ITT FW114 biplanar diode and a Tektronix 519 oscilloscope. The absence or presence of internal damage within the sample was determined by viewing with the unaided eye, using side lighting from a low power He-Ne laser. A visible spark inside the crystal was noted whenever internal damage was produced. Following each pulse the sample was translated such that an undamaged sample volume was in position for each laser pulse. The peak power density threshold values for the MM and TEM_{oo} lasers are shown in Table I for different directions of laser propagation and polarization. The notation, P(xy), indicates that the laser was propagating along the x-crystallographic direction and was polarized parallel to the y-crystallographic direction. The damage threshold values shown in Table I indicate a propagation and polarization directional dependence for the MM laser. The threshold values for the TEM_{oo} laser were independent of propagation and polarization.

The damage threshold values of Table I were estimated as follows: For a given propagation and polarization direction, the peak power density for each pulse was recorded as to whether damage was produced or not. The $+5GW/cm^2$ values correspond to the damage power density above which 80% of the laser pulses produced damage. Below the $-5GW/cm^2$ values, 80% of the laser pulses did not produce damage. The damage threshold peak power density is the median of these two values. The $\pm 5GW/cm^2$ deviation in Table I was recorded directly for each set of measurements and is not the result of a weighted statistical analysis. For the z-propagation

Table I. Internal damage threshold values in quartz for the multimode and TEM_{oo} lasers. P(xy) indicates the peak power density for a laser pulse incident in the x-crystallographic direction and polarized along the y-direction.

Multimode Laser

$P(xy) = 34 \pm 5$ GW/cm^2
$P(xz) = 130 \pm 5$ GW/cm^2
$P(yx) = 63 \pm 5$ GW/cm^2
$P(yz) = 47 \pm 5$ GW/cm^2
$P(zx) = 80 \pm 5$ GW/cm^2
$P(zy) = 80 \pm 5$ GW/cm^2

TEM_{oo} Laser

$P(ij) = 28 \pm 5$ GW/cm^2
$i,j = x, y, z$

direction, about 75 data points were used. About 30 data points were used for the x- and y-propagation direction measurements. A proper statistical analysis would assign a smaller variance to the threshold value for the z-propagated damage than for the x- or y-directions. It should be noted that the threshold value for the TEM_{oo} laser, P(ij) = 28 ± 5GW/cm^2, falls within the range of values quoted by Olness[14] (13-30GW/cm^2) for damage produced by a "single spatial mode" ruby laser.

The damage threshold peakpower density values were computed using the measured laser peak power and the time-integrated beam diameter of Fig. 5. For the TEM_{oo} laser, the time integrated beam diameter is approximately the same as the instantaneous values,[12] and the space integrated pulse duration is approximately the same as the local values. Therefore, the value listed in Table I for the TEM_{oo} laser is an accurate representation of the threshold. For the MM laser, however, the pulse is irregular in time and space such that the values given in Table I for the MM laser can only be considered as relative and should not be compared with the TEM_{oo} threshold values. However, the relative values of the MM laser data are accurate because of the "80% points" method of recording.

No evidence of self-trapping tracks was observed for any of the damage regions produced by either laser in these experiments in quartz. Under other conditions, the critical power[15] required for catastrophic self-focusing may be achieved and we could produce self-trapped tracks in crystalline quartz. If possible, self-trapping which complicates and sometimes confuses the picture of laser damage[16] should be avoided so that the basic mechanisms of laser damage may be studied and compared.

Given in Table II are the ratios of the propagation velocities of elastic waves (acoustic phonons) in crystalline quartz. v(zx) is the velocity of a wave propagating in the z-direction and polarized along the x-direction. The velocities were calculated in the usual manner[17] using published elastic constant data for quartz. Also listed are ratios of the MM damage threshold peak power densities of Table I. One can see a strong dependence of the ratios of the MM laser damage threshold values on the acoustic phonon propagation in quartz.

The following phenomenological model has been developed to explain the damage mechanism in quartz for the two lasers. Radiation incident on

Table II. Ratios of the acoustic wave propagation velocities and multimode laser damage values in quartz. v(zx) is the velocity of a wave propagating in the z-direction and polarized in the x-direction.

	v(zx)	v(yx)	v(yz)
v(zy)	1.0	0.83	0.80

	P(zx)	P(yx)	P(yz)
P(zy)	1.0	0.84	0.75

a dielectric sample such as quartz primarily interacts with the electrons and the electrons in turn interact with the lattice. Under some conditions the incident radiation can also interact directly with the lattice through electrostriction.[18] For either the direct or indirect radiation-lattice interaction, the ions will be set in motion with a given amplitude. The magnitude of the amplitude will depend on the amount of energy pumped into the lattice from the incident field. For proper input conditions the amplitude of the ionic motion may reach a threshold value at which the ionic bonds are broken resulting in the observed internal damage. The increase in the amplitude of the ionic vibrations in the crystal due to the amplification of acoustic phonon motions depends directly on crystallographic direction and not on the laser mode structure. The internal damage patterns would, therefore, be expected to depend on the direction of propagation and not on the type of laser used. Figure 6 shows typical damage patterns produced by the MM lasers. When the laser was propagating along either x- or y-crystallographic direction, a cross was observed in the damage cross-section as shown in Fig. 6a. A circular damaged cross-section is seen in Fig. 6b when the laser is fired into the z-direction of the crystal. The damage patterns in both cases can be correlated with the directional dependence of sound velocities.[19] The damage patterns produced by the TEM_{oo} laser have similar directional dependence with fracture patterns about ten times smaller.

The difference in damage thresholds in the two lasers may be explained as follows. The temporal and spatial variation of the TEM_{oo} laser field is smooth. This type of light pulse interacts primarily with the electrons. The efficiency of this interaction is quite independent of crystallographic direction for insulators such as quartz, and thus the damage threshold value would be independent of the propagation and polarization directions of the incident laser pulse as given in Table I. The strong spatial and temporal gradients present in the output profiles for the MM laser on the other hand can modulate the ionic motion by electrostrictive interaction. This modulation has components in the same frequency and wave vector range as the zone-center acoustic phonons of the crystal and as a result laser energy may also be absorbed directly and critically by the lattice from the incident pulse. Because the excitation

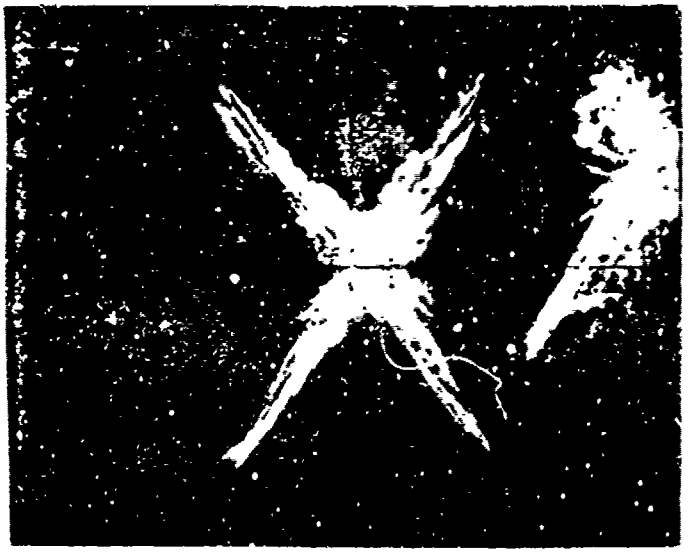

(6a). Either the x or y crystallographic direction.

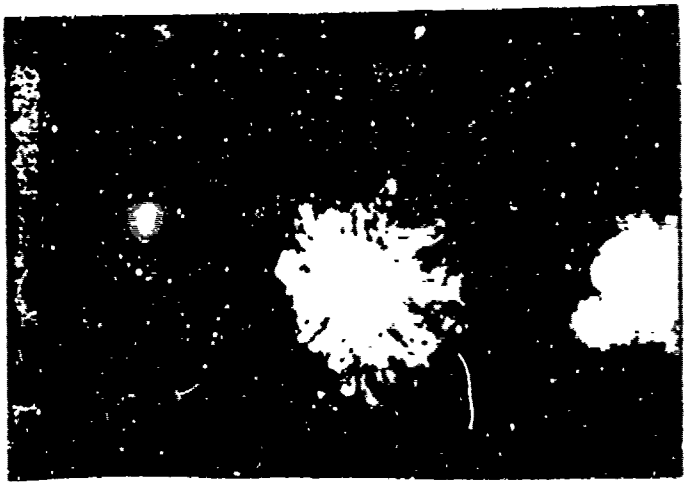

(6b). z-direction propagation.

Fig. 6. Typical damage patterns produced by the MM laser for different propagation directions in quartz. (a) The laser was propagating along either the x or y crystallographic direction. (b) z-direction propagation. The fracture patterns produced by the TEM_{00} laser are similar and are about ten times smaller

of the acoustic wave in this case results directly from the strong spatial and temporal intensity gradients of the propagating MM laser pulse, its propagation and polarization is dictated by the laser beam. As the ionic motion depends on the crystallographic bonding directions, the efficiency of this interaction and the MM laser damage threshold values would be dependent on crystallographic directions (Table I). The existence of electrostrictive interactions may also cause self-focusing of the laser beam in solids. It should be noted that self-focusing requires a critical beam intensity and the direct coupling between the radiation and the acoustic wave in our model depends only on the strong intensity gradients of the MM laser pulse. It can be estimated[15] that our laser intensity was below the critical value for catastrophic self-focusing but the intensity gradient for the MM laser was strong enough to excite acoustic waves of catastrophic amplitudes resulting in fracture within the crystal.

The details of the effects of laser mode structure on damage will be published elsewhere.[19] In addition, we have also examined the surface damage patterns produced by the TEM_{oo} and MM lasers. This is shown in Fig. 7. Contrary to the internal damage, the laser mode structure has a pronounced effect on the surface damage patterns as well.

IV. EVOLUTION OF MICROSCOPIC DAMAGE

Primary goal of this as well as most laser damage programs had been to determine the origin of the damage. The research program described here attempted to determine the conditions under which the macroscopic damage could evolve from the microscopic damage. From the experiment described in Section II it was concluded that if a memory of microscopic damage existed in crystalline quartz, it would have a short lifetime. To pursue the memory and evolution ideas further the following experiments were performed. (1) The incident and transmitted radiation were monitored for a laser pulse with peak power 80% of the macroscopic threshold value. Both the multimode and TEM_{oo} laser were used for this experiment. (2) The incident and 90° scattered radiation were monitored. For this experiment only the TEM_{oo} laser was used, but samples of crystalline quartz, fused silica, and Nd-laser glass were used.

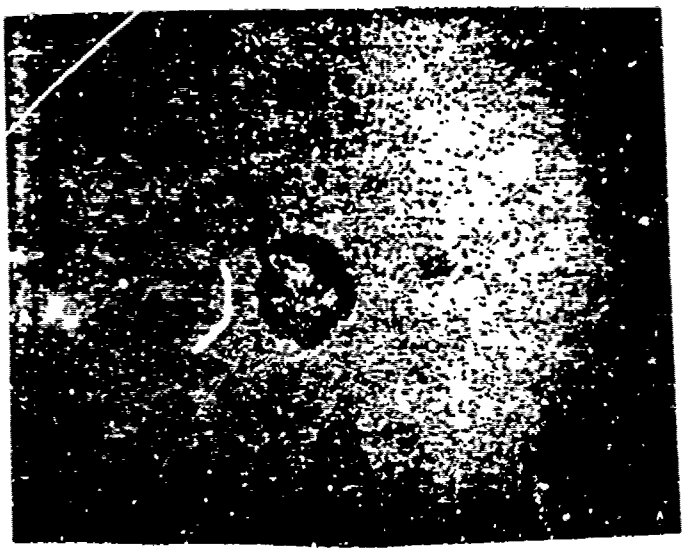

(7a). TEM_{oo} Laser

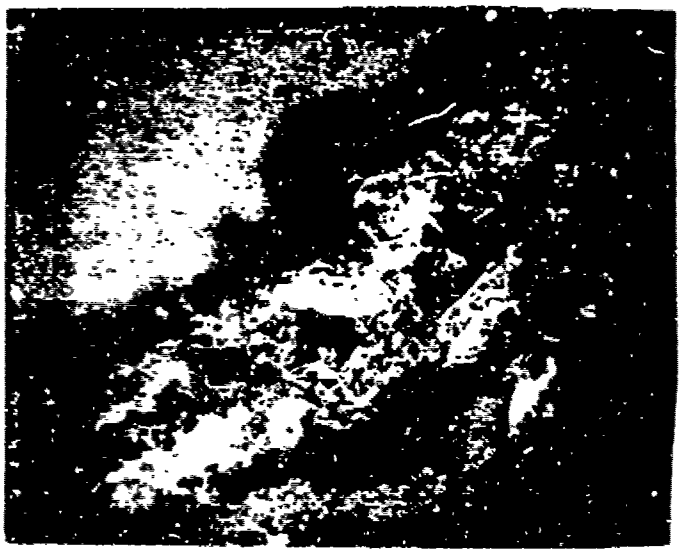

(7b). Multimode Laser

Fig. 7. Microphotographs of the surface damage produced by the two lasers.

For the transmission experiment, the incident and transmitted pulses were recorded by a single photodiode (FW114) and oscilloscope (Tektronix 519). The incident pulse was optically or electrically delayed relative to the other pulse, thus permitting the two pulses to appear on a single oscilloscope trace. For this experiment the optical and electrical delay schemes gave equivalent results. Large fluctuations were observed in the ratio of the transmitted to incident power using the multimode laser. These fluctuations were due to the complex mode structure and poor reproducibility of the laser pulse.[20] Using the TEM_{oo} laser, the fluctuations in the data were negligible. Shown in Fig. 8 is the ratio of the transmitted energy (i.e. the area under the pulse) to the incident energy plotted as a function of the number of laser pulses incident in a particular sample volume. The TEM_{oo} laser pulses corresponding to these data were each at about 80% of the macroscopic damage threshold value. The solid line in the figure is a least-squares fit of the data points to a sloping straight line. The data were also fitted to a constant value but the resulting "confidence of fit" was appreciably greater for the line shown. Second and third order polynomials were also fitted to the data but the confidence was about the same as for the sloping straight line. The large ratio value for pulse number 13 is probably due to a malfunction of the laser. For those places where no data are given, the oscilloscope did not function properly so that no traces were recorded. The error bar shown in the figure was determined from the reproducibility of reading the areas under the oscilloscope traces.

From the decrease in the energy ratios of Fig. 8 it is concluded that a cumulative effect of microscopic damage was observed. The evolution of macroscopic effects from these microscopic effects was not observed before the determination of the experiment (20 laser pulses).

The data of Fig. 8 were also analyzed by searching for nonlinearities in the instantaneous powers of the incident and transmitted beams for a given laser pulse. Shown in Fig. 9 is a typical plot of the instantaneous incident power, P_i, as a function of the corresponding transmitted power, P_t, for a typical data point of Fig. 8. The solid curve represents a least-squares fit of the data points to a quadratic curve. The confidence

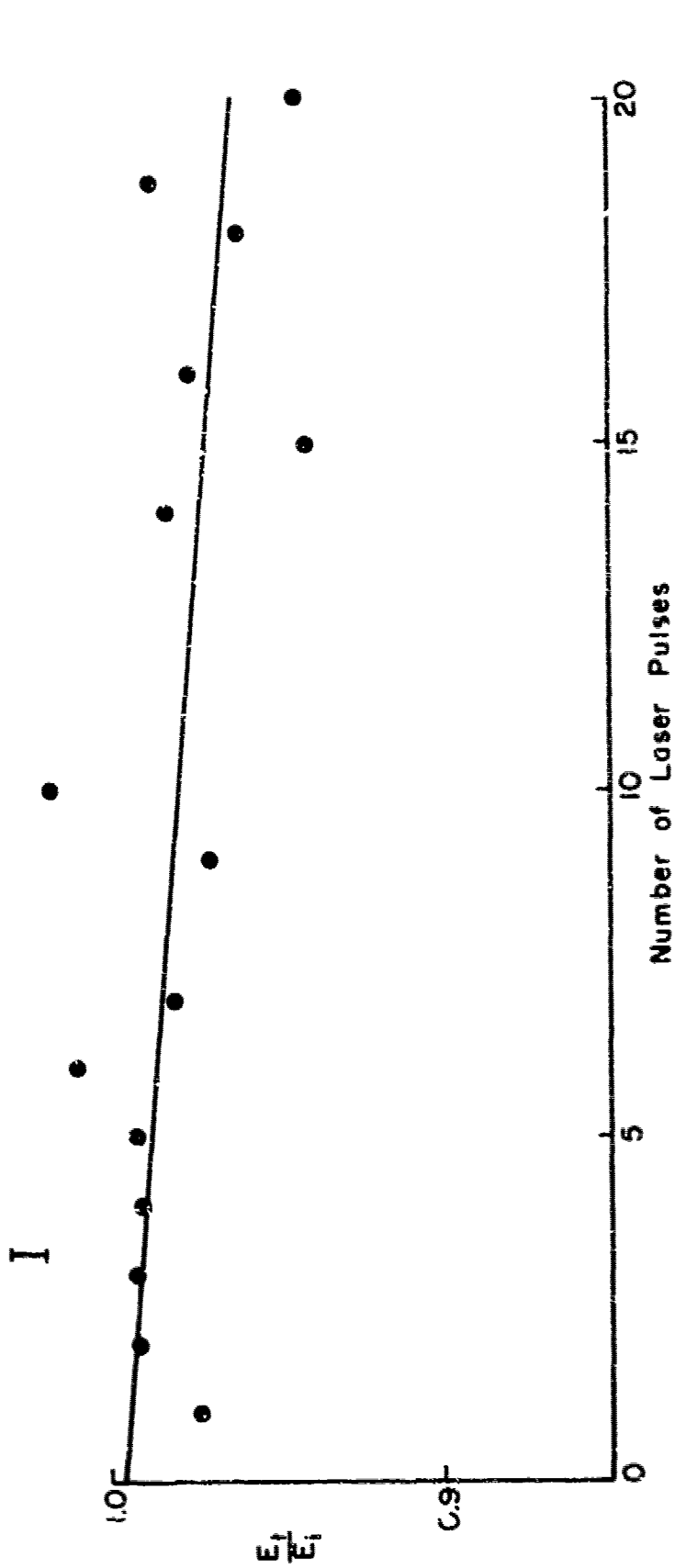

Fig. 8. Ratio of transmitted energy to incident energy as a function of the number of laser pulses for TEM_{00} laser.

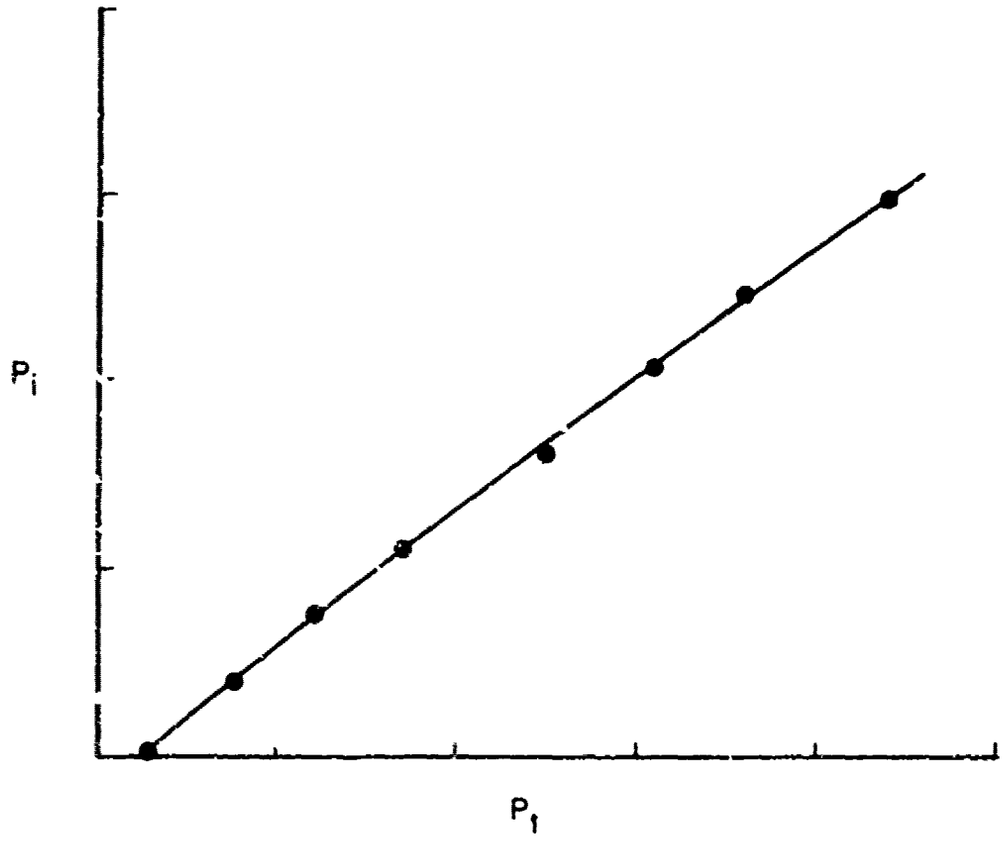

Fig. 9. Instantaneous incident power versus transmitted power for typical TEM_{oo} laser pulse.

of this fit was better than for a straight line fit. This quadratic dependence would indicate that during the lifetime of the laser pulse a slight nonlinearity, perhaps due to a change in the refractive index of the sample, had been introduced by the incident laser. No data were available where macroscopic damage was produced.

For the 90° scattering experiment it was theorized that, if cumulative effects were present, the scattered light, starting from a very low level, should increase by a small amount with each successive laser pulse and would be expected to increase suddenly when catastrophic damage was produced. This sudden change in the amount of scattered light would thus be evidence of the evolution of microscopic into macroscopic damage. To test this hypothesis, the TEM_{oo} laser was used to irradiate samples of crystalline quartz, fused silica and Nd-laser glass. Shown in Figs. 10 and 11 are plots of the ratio of the scattered to incident power as a function of the number of laser pulses for samples of crystalline quartz and fused silica, respectively. The peak power of each pulse was about 80% of the catastrophic damage threshold value. For both samples, changes in the 90° scattered light are inconclusive. For the Nd-laser glass samples, the scattered light was not detected because of the large absorption in the glass. For each sample, measurements were made of the 90° scattered radiation for each successive laser pulse until the sample developed catastrophic damage. Within the accuracy of Figs. 10 and 11 evidence of microscopic damage is inconclusive. This type of experiment is apparently less sensitive than the forward scattering experiment.

V. SUMMARY AND DISCUSSION

An important conclusion of this research is that the mechanism governing the onset of laser-produced damage in solids depends, in a critical way, on the spatial and/or temporal gradient of the interaction strength across the focal volume. Differences in macroscopic damage threshold were measured for the TEM_{oo} and the multimode laser. Due to the strong spatial and temporal gradients of the multimode laser beam, the electrostrictive interaction provides a direct way of feeding energy to the

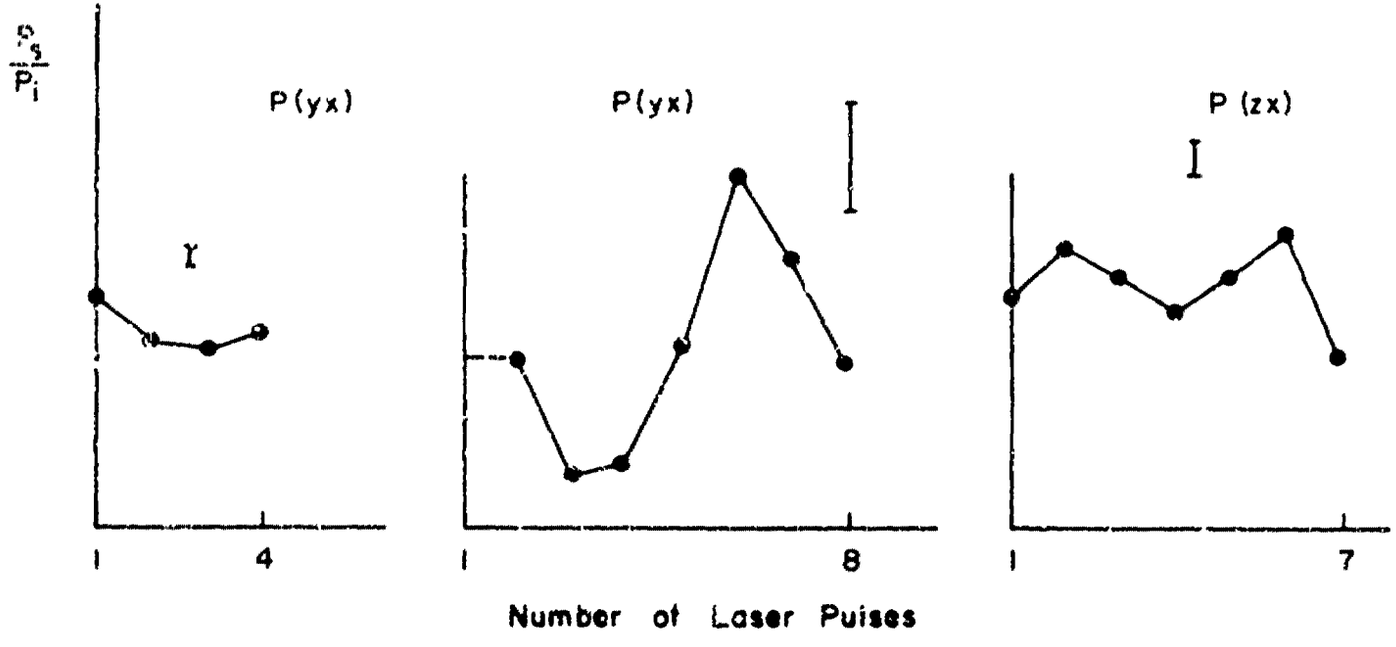

Fig. 10. The ratio of the 90° scattered power to incident power vs. pre-damage shot number for crystalline quartz.

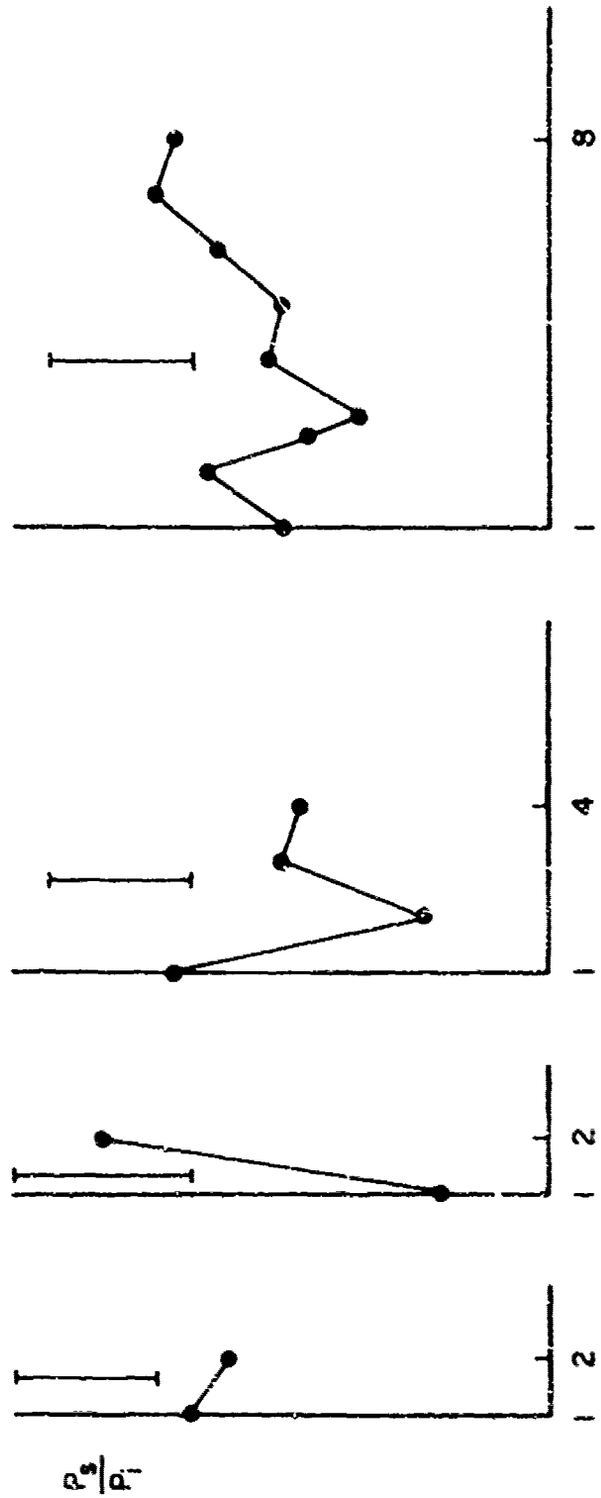

Fig. 11. The scattering ratios for fused quartz.

acoustic phonons in the crystal and thus resulting in a directional dependent threshold values. For the TEM_{oo} laser, the incident radiation can only interact with electrons, and unless catastrophic damage occurs, phonons in the crystal will not be significantly perturbed, thus accounting for not observing changes in Raman line position or linewidth in microscopically damaged quartz. For one experiment the cumulative effects of microscopic damage were observed in crystalline quartz. Other experiments designed to detect cumulative effects were not affirmative indicating that these measurements were not as sensitive as first assumed.

The technique of light scattering as a diagnostic tool for laser induced microscopic damage can be effective if used under proper conditions. To be completely successful it is necessary to differentiate laser-induced effects from normal light scattering effects. The results of this research program indicate that light scattering measurements can provide information about damage and may be the only tool to diagnose the true mechanism for laser-induced damage in solids. Further investigations on the differences between amorphous and crystalline materials, such as quartz and fused quartz samples, in terms of laser produced damage should be continued.

REFERENCES

1. A. J. Glass and A. H. Guenther, "Damage in Laser Glass," ASTM Symposium, 1969, Special Tech. pub. 469.
2. A. J. Glass and A. H. Guenther, "Damage in Laser Materials," ASTM Symposium, 1970, NBS Special pub. 341.
3. A. J. Glass and A. H. Guenther, "Damage in Laser Materials - 1971," ASTM Symposium, 1971, NBS Special pub. 356.
4. Y. D. Harker, C. Y. She and D. F. Edwards, "Stress-Dependent Raman Frequency and Linewidth in α-Quartz," Appl. Phys. Letters 15, 272 (1969).
5. D A. Kleinman and W. G. Spitzer, "Theory of the Optical Properties of Quartz in the Infrared," Phys. Rev. 125, 16 (1962).
6. Y. D. Harker, C. Y. She and D. F. Edwards, "Raman Spectra of α-Quartz Under Uniaxial Stress," Jour. Appl. Phys. 41, 5274 (1970); Y. D. Harker, C. Y. She and D. F. Edwards, "Effect of Uniaxial Stress of Vibrational Modes in α-Quartz," Tech. Rept. AFCRL - 69 - 0445, U.S. Air Force (1969).
7. J. D. Masso, "Raman Scattering in α-Quartz," Ph.D. Thesis, Colorado State University (1970).
8. C. M. Stickley, H. Miller, E. E. Hoell, C. C. Gallagher and R. A. Bradbury, "Color Centers and Ruby-Laser Output-Energy Degradation," J. Appl. Phys. 40, 1792 (1969).
9. A. L. Schawlow, D. L. Wood, and A. M. Clogston, "Electronic Spectra of Exchange-Coupled Ion Pairs in Crystals," Phys. Rev. Letters 3, 271 (1959).
10. R. C. Powell, B. DiBartolo, B. Birang, and C. S. Naiman, "Fluorescence Studies of Energy Transfer Between Single and Pair Cr^{3+} Systems in Al_2O_3," Phys. Rev. 155, 296 (1967).
11. D. F. Edwards, Y. D. Harker, J. D. Masso and C. Y. She, "Diagnostic and Evidence of Pre-catastrophic Damage in Transparent Solids," ASTM STP 469, 128 (1969).
12. G. L. McAllister, M. M. Mann and L. G. De Shazer, "Transverse-Mode Distortions in Giant-Pulse Laser Oscillations," IEEE J. of Quantum Electronics QE-6, 44 (1970).
13. D. F. Edwards, C. Y. She, J. D. Masso, Y. D. Harker and H. C. Schade, "Raman Scattering in Microscopically Damaged Quartz," in Damage in Laser Materials, A. J. Glass and A. H. Guenther ed., NBS Special pub. 341, 97 (1970).

14. D. Olness, "Laser-Induced Breakdown in Transparent Dielectrics," J. Appl. Phys. 39, 6 (1968).

15. E. L. Dawes and J. H. Marburger, "Computer Studies in Self-Focusing," Phys. Rev. 179, 862 (1969).

16. E. S. Bliss, "Pulse Duration Dependence of Laser Damage Mechanisms," Second ASTM Symposium on Damage in Laser Materials, NBS Special pub. 341, 105 (1970).

17. C. Kittel, Introduction to Solid State Physics, 3rd Ed. (John Wiley and Sons, New York, 1968).

18. Edwin L. Kerr, "Transient and Steady-State Electrostrictive Laser Beam Trapping," IEEE Jour. Quantum Electronics QE-6, 616 (1970).

19. V. G. Draggoo, C. Y. She, G. L. McAllister and David F. Edwards, "Effects of Laser Mode Structure on Damage in Quartz," IEEE Quantum Electronics, Feb. 1972 (to be published).

20. David F. Edwards, C. Y. She, V. G. Draggoo, T. W. Broberg and G. L. McAllister, "Investigation of Cumulative Effects in Microscopically Damaged Quartz," Third ASTM Symposium on Laser Damage, NBS Special pub. 356, 24 (1971).

CONTRIBUTING SCIENTISTS AND ENGINEERS

1. David F. Edwards, Professor of Electrical Engineering and Physics, Principal Investigator.
2. Chiao-Yao She, Associate Professor of Physics, Investigator.
3. Sanford Kern, Associate Professor of Physics, Investigator.
4. G. L. McAllister, Assistant Professor of Electrical Engineering, Consultant.
5. Y. D. Harker, Ph.D. Student.
6. Jon D. Masso, Ph.D. Student.
7. T. W. Broberg, Ph.D. Student.
8. H. C. Schade, Graduate Student.
9. V. G. Draggoo, Graduate Student.

PUBLICATIONS

Resulting from Partial Sponsorship of the Contract

1. Y. D. Harker, Jon D. Masso and David F. Edwards, Appl. Opt. 8, 2563 (1969).
2. David F. Edwards, Jon D. Masso, Y. D. Harker and C. Y. She, in Damage in Laser Glass, A. J. Glass and A. H. Guenther ed., Special Technical publication, Amer. Soc. Testing and Materials STP 469, 128 (1969).
3. Y. D. Harker, C. Y. She and David F. Edwards, Appl. Phys. Letters 15, 272 (1969).
4. Y. D. Harker, C. Y. She and David F. Edwards, Technical Report AFCRL - 69 - 0445, U.S. Air Force (1969).
5. J. D. Masso, C. Y. She and David F. Edwards, Phys. Rev. B1, 4179 (1970).
6. David F. Edwards, C. Y. She and Jon D. Masso, Bull. Amer. Phys. Soc. 15, 297 (1970).
7. C. Y. She, Jon D. Masso and David F. Edwards, Bull. Amer. Phys. Soc. 15, 372 (1970).
8. David F. Edwards, C. Y. She and Y. D. Harker, Bull. Amer. Phys. Soc. 15, 810 (1970).
9. David F. Edwards, C. Y. She, Jon D. Masso, Y. D. Harker and H. C. Schade, in Damage in Laser Materials, A. J. Glass and A. H. Guenther ed., U.S. Dept. of Commerce, NBS Special publication 341, 97 (1970).
10. David F. Edwards and C. Y. She, "Evidence of Laser-Induced Pre-catastrophic Damage in Quartz," Presentation, International Quantum Electronics Conference, Kyoto, Japan, Sept. 1970.
11. Y. D. Harker, C. Y. She and David F. Edwards, J. Appl. Phys. 41, 5274 (1970).
12. C. T. Meneely, C. Y. She and David F. Edwards, J. Mol. Spec. 39, 73 (1971).
13. C. Y. She, Jon D. Masso and David F. Edwards, J. Phys. Chm. Solids 32, 1887 (1971).
14. V. G. Draggoo, "Laser Induced Damage in Quartz," M.S. Thesis, Colorado State University.
15. C. Y. She, T. W. Broberg and David F. Edwards, Phys. Rev B4, 1580 (1971).

16. David F. Edwards, C. Y. She, V. G. Draggoo, T. W. Broberg and G. L. McAllister, in Damage in Laser Materials - 1971, A. J. Glass and A. H. Guenther ed., U.S. Dept. of Commerce, NBS Special publication 356, 24 (1971).

17. V. G. Draggoo, C. Y. She, G. L. McAllister and David F. Edwards, IEEE J. Quan. Elect., Febr. 1972 (to be published).

Unclassified

Security Classification

DOCUMENT CONTROL DATA - R & D

(Security classification of title, body of abstract and indexing annotation must be entered when the overall report is classified)

1 ORIGINATING ACTIVITY (Corporate author) Colorado State University Fort Collins, Colorado 80521	2a REPORT SECURITY CLASSIFICATION Unclassified 2b GROUP

3 REPORT TITLE

LASER PRODUCED DAMAGE IN TRANSPARENT SOLIDS

4 DESCRIPTIVE NOTES (Type of report and inclusive dates)
Scientific, Final: (1 March 1969 - 30 September 1971)

Approved: 22 March 1972

5 AUTHOR(S) (First name, middle initial, last name)
David F. Edwards
C. Y. She

6 REPORT DATE February 1972	7a TOTAL NO OF PAGES 39	7b NO OF REFS 20
8a CONTRACT OR GRANT NO F-19628-69-C-0197 b PROJECT, TASK, AND WORK UNIT NO 4645-07-01 c DOD ELEMENT 62403F d DOD SUBELEMENT 634645	9a ORIGINATOR'S REPORT NUMBER(S) AFCRL-72-0143	

9b OTHER REPORT NO(S) (Any other numbers that may be assigned this report)

10 DISTRIBUTION STATEMENT

A-Approved for public release; distribution unlimited.

11 SUPPLEMENTARY NOTES TECH, OTHER	12 SPONSORING MILITARY ACTIVITY Air Force Cambridge Research Laboratories (OP) L. G. Hanscom Field Bedford, Massachusetts 01730

13 ABSTRACT

The mechanism governing the onset of laser-produced damage in solids was found to depend, in a critical way, on the spatial and/or temporal gradient of the interaction strength across the focal volume. As a result, the threshold values of damage produced by a multimode laser as well as the internal damage patterns depend strongly on the laser propagation and polarization directions.

In the forward scattering experiment, the cumulative effects of microscopic damage were observed in crystalline quartz. Other experiments designed to detect cumulative effects were inconclusive. Various light scattering spectroscopy as a diagnostic tool for laser-produced damage studies were investigated.

DD FORM 1473

Unclassified

Security Classification

Unclassified
Security Classification

14 KEY WORDS	LINK A		LINK B		LINK C	
	ROLE	WT	ROLE	WT	ROLE	WT
Laser Damage						
Transparent Solids						
Directional Dependence						
Light Scattering						

Unclassified
Security Classification